CO_2 Capture Using Hydrated Lime: A Study on the Role of Water Evaporation

Natalia. Vidal de la Peña[a]*, Séverine Marquis [b], Stéphane Jacques [b], Dominique Toye[a] and Grégoire Léonard [a]

[a] University of Liège, Department of Chemical Engineering, PEPs—Products, Environment, and Processes, Liège, Belgium
[b] Centre Pierre et Terre(CTP), Chaussée d4antoing, 55, 7500 Tournai, Belgium

* Corresponding Author: nvidal@uliege.be, Bât. B6C PEPs - Products, Environment, and Processes, Quartier Agora, allée du six Août 11, 4000 Liège Sart Tilman, Belgium, +320492368634

Abstract

The construction industry generates 38% of Europe's total waste, highlighting the need for improved sustainability. This study proposes a mathematical model, implemented in COMSOL Multiphysics 6.2,which incorporates the three primary phenomena occurring during the carbonation of hydrated lime: chemical reaction, diffusion, and water evaporation. Water plays a crucial role in this process, and this work highlights its influence by incorporating rigorous water balances. During carbonation, most of the water in the system evaporates due to the exothermic nature of the reaction. However, a portion of the water becomes physically adsorbed onto the material and remains non-evaporable. A linear equation correlating the evaporation ratio with the total carbon content during the carbonation process is provided. Additionally, the influence of liquid water saturation is considered in both the reaction kinetics and the diffusion phenomena. Experimental results for total carbon uptake and the mass of evaporated water are presented and compared with model predictions, elucidating the effects of the initial water-to-solid ratio and carbon dioxide flow rates. An optimization of initial water-to-solid ratios is provided, achieving an optimal value of 0.3 for the carbonation of hydrated lime. In conclusion, this study contributes to a deeper understanding of CO_2 capture through mineral carbonation, supporting efforts to enhance sustainability in the construction sector.

Keywords: ex-situ mineral carbonation, mineral wastes, COMSOL Multiphysics, diffusion, kinetics

1. Introduction

Nowadays, the continuous pursuit of human well-being and the improvement of quality-of-life leads to an increasingly high consumption of natural resources, leading to their exhaustion and generating waste and pollutants that are difficult to manage. This is evident in the construction industry, as it is one of the main contributors to European waste streams, accounting for 38% of the total European waste in 2022, as reported by Eurostat (2022). In addition, this industry significantly contributes to CO_2 European emissions, producing around 0.05 Gt of CO_2 in 2022 [1]. Taking into consideration the increasing trend of the presence of CO_2 in the atmosphere, the EU established a Green Deal to achieve carbon neutrality by 2050 and a reduction of 55% in the CO_2 emissions by 2030[2]. To this end, the EU is focusing on improving energy efficiency, the use of renewable energy and CCUS (Carbon Capture, Utilization and Storage) technologies.

In response to this challenge, the Walloon-Region funded project Mineral Loop was established [3]. The project's objective is to design, develop, install, and operate an industrial pilot unit capable of transforming mineral construction waste into secondary products that can be reused across various application sectors. This project is a step ahead considering that around 44% of the waste streams in the construction sector concern mineral wastes [4]. Within the scope of the Mineral Loop project, the mineral carbonation of hydrated lime is proposed as a means of capturing CO_2. The hydrated lime is selected as a benchmark material due to its prevalence in mineral waste, such as hydrated lime-based cementitious residues [5]. Currently, mineral carbonation processes primarily focus on the CO2 capture and underground storage[6]. However, in sectors such as construction, developing methods

to control and optimize the carbonation of mineral residues for their reuse could significantly contribute to the circular economy of the industry.

Mineral carbonation can be categorized in two methods: in-situ and ex-situ. In-situ mineral carbonation occurs underground such as the reaction between landfilled hydrated lime-based waste and ambient or injected carbon dioxide. In contrast, ex-situ mineral carbonation involves the collection, preparation, and subsequent treatment of residues in a controlled environment [7]. In this study, the carbonation of calcium hydroxide is classified as ex-situ mineral carbonation, as it is conducted in a reactor where the CO_2 flow is regulated, and the material is prepared prior to the initiation of the process. Moreover, ex-situ mineral carbonation can be conducted through direct or indirect processes. This study focuses on gas-solid direct carbonation, which involves the reaction between carbonatable materials and CO_2 in a single stage, avoiding the several stages required in the indirect carbonation processes, such as e.g., calcium ions extraction into a liquid solvent [7]. In summary, in this context, the hydrated lime carbonation is categorized as an ex-situ direct mineral carbonation and the simplified carbonation reaction that will be modelled is expressed as follows.

$$Ca(OH)_2\,(s) + CO_2(g) \rightarrow CaCO_3\,(s) + H_2O(l) \qquad \Delta H°_{298\,K} = -109\ kJ/mol \tag{1}$$

Although the overall carbonation expressed in the Equation (1) appears to be simple, it involves several steps. The reaction occurs entirely in the liquid phase between Ca^+ and OH^- ions, which originate from the dissolution of $Ca(OH)_2$ and CO_2 in water [8–10]. Due to these dissolution steps, water is essential to initiate the carbonation process [11,12]. This necessity gives rise to the water-to-solid ratio parameter (w_s^0), which is the ratio between the mass of water initially added and the initial mass of solid material that will be carbonated. An insufficient water-to-solid ratio can result in an inadequate amount of water to dissolve the solid, thereby preventing the reaction from occurring [10,12,13]. Conversely, an excess of water may lead to slow diffusion of CO_2 through the liquid film, slowing down and possibly preventing the carbonation process. Additionally, excessive water can cause agglomeration, forming paste-like clusters that hinder homogenization of the mixture [12]. The study done by M. Thiery et al. (2015) highlighted that the optimal water-to-solid ratio for the carbonation of a model material was found to be around 0.45 [12]. The high sensitivity of hydrated lime to water makes the optimization of this parameter essential.

In our previous work, the influence of water was treated in a simplified manner by accounting for its effect on the reaction and diffusion phenomena, without considering evaporation, despite experimental evidence highlighting its significance [8]. These observations motivated a more in-depth investigation into the dynamics of water evaporation. During the hydration of cementitious materials, water is generally classified into two categories: non-evaporable and evaporable water. Non-evaporable water is chemically bound within the material, typically located between the hydrate layers. In contrast, evaporable water includes capillary water present in the pore structure and physically adsorbed water, retained through hydrogen bonding with hydroxide phases in both the internal and external layers of the hydrated material [14,15].

Following with the evaporation process, the study by Ö. Cizer et al. (2012) demonstrated that water evaporation alters both the phase and morphology of calcium carbonate. One effect observed was that rapid evaporation can induce shrinkage cracks, which affect the diffusion of carbon dioxide through the material and consequently influence the kinetics of the carbonation process [13]. Building upon the hypothesis proposed by Ö. Cizer et al. (2012), M. Thiery et al. (2015), and our previous work, the proposed mathematical model accounts for the influence of water within the material in the three key phenomena (reaction, diffusion, and evaporation) by introducing the liquid water saturation and water-to-solid ratio parameters[8].

This study presents a comprehensive analysis of water behavior in the carbonation process of hydrated lime, integrated into a mathematical model implemented in COMSOL Multiphysics. By providing a deeper understanding of the coupling and interdependency of the fundamental physicochemical phenomena involved in solid carbonation, the model contributes to the development of sustainable practices aligned with the principles of the circular economy in the construction sector.

2. Materials and methods

2.1. Experimental work and material characteristics

A total of 8 carbonation experiments were conducted using pure hydrated lime with the purpose of analyzing the behavior of this material facing the carbonation process and the water balance of the system. The main goal of doing these experiments was to understand the impact of some physical and controllable parameters such as the initial-water-to-solid ratio and the carbon dioxide flowrate. These experiments are later used to validate the mathematical model proposed.

2.2. Experimental procedure and calculations associated

Carbonation experiments were conducted using pure hydrated lime, a fine powder with an initial particle diameter of 35.5 µm. To characterize the initial material, total carbon analysis was performed, yielding a carbon content of 0.5043%. This measurement was conducted using a CS744 carbon/sulfur analyzer. For each analysis, 500 mg of dried sample was introduced into the instrument and combusted in an oxygen stream via radio frequency induction heating. During combustion, carbon was oxidized to CO_2, which was subsequently quantified using a non-dispersive infrared (NDIR) detector, enabling precise determination of the total carbon content.

Following characterization, the hydrated lime was manually mixed with water in accordance with the target initial water-to-solid (w_s^0) ratio for each experiment. The initial water-to-solid ratio parameter corresponds to the mass of water initially added divided by the initial mass of solid. The mixture was allowed to homogenize for 2 h to ensure uniform water diffusion throughout the material. After homogenization, the mixture was transferred into an aluminum cup with a base diameter of 70 mm, a top diameter of 83 mm, and a height of 25 mm. The aluminum cup was placed inside a semi-batch continuous reactor with a total volume of 1.4 L. In the initial stage, the reactor was completely filled with air, after which pure carbon dioxide was continuously introduced for the designated carbonation period. The experimental setup is presented in Figure 1. Figure 1a shows a schematic diagram of the setup, while Figure 1b provides a photograph of the reactor and the aluminum cup containing the material prepared for carbonation.

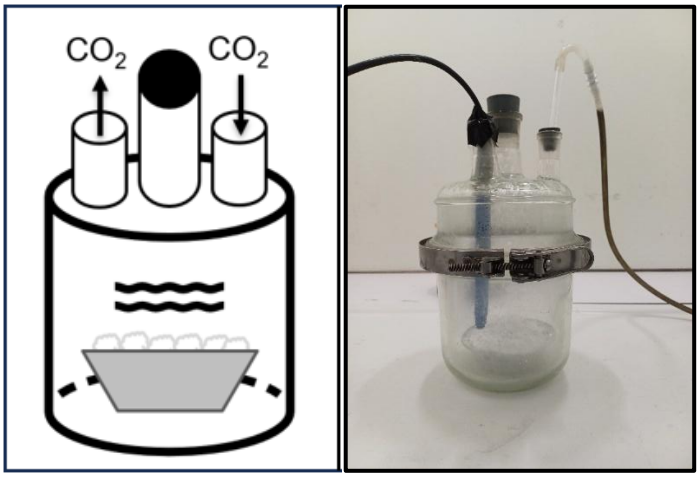

Figure 1. (a) Scheme of the experimental set-up [8]. (b) Experimental set-up.

A total of eight experiments conditions were tested, each performed in duplicate to ensure reproducibility and reliability of the results. In previous work, carbonation was investigated using initial water-to-solid ratios ranging from 0.1 to 0.4. In the present study, this range was extended from 0.1 to 0.6 to explore a broader set of reaction conditions. The selected w_s^0 ratio range was based on values reported in the literature, which indicate an optimal ratio of approximately 0.45 [12]. Table 1 summarizes the experimental plan and corresponding results for the carbonation tests. It includes key parameters such as the initial w_s^0 ratio, calculated as the mass of water added

prior to carbonation divided by the initial mass of solid material (m_s^0). The table also reports the carbon dioxide flow rate, the carbonation duration, the mass of water remaining in the solid matrix after carbonation (m_{wm}), and the total carbon content measured after each experiment.

Table 1. Experimental conditions and results: initial water-to-solid ratio (w_s^0), carbonation time, carbon dioxide flow rate, initial solid mass (m_s^0), mass of water remaining in the solid matrix after carbonation (m_{wm}), and total carbon content (CT_{exp})

Carbonation experiment	w_s^0 (g_{H2O}/g_s)	CO_2 flow rate (mL/min)	Carbonation time (min)	m_s^0 (g)	m_{wm} (g)	TC_{exp}(g_C/g_s)
1	0.1	100	45	54.95	5.67	4.74
2	0.3	100		45.32	12.34	7.88
3	0.4	100		44.88	16.53	6.24
4	0.6	100		47.89	28.06	4.33
5	0.1	200	45	55.06	5.95	6.88
6	0.3	200		47.45	12.57	9.03
7	0.4	200		47.12	18.06	8.47
8	0.6	200		44.64	25.54	4.24

Regarding the experimental conditions and results presented in Table 1, several important observations can be made concerning the influence of water content and carbon dioxide flowrate on the carbonation process. Analysis of the total carbon content reveals that, as previously discussed, the initial water-to-solid ratio has a direct impact on the extent of carbonation. Low w_s^0 ratios (e.g., 0.1) result in significantly lower total carbon values compared to experiments conducted with higher w_s^0 ratios, such as 0.3 or 0.4. However, high w_s^0 ratios appear to hinder the carbonation process. This effect is particularly evident in experiments using a w_s^0 of 0.6, where total carbon content is markedly reduced. This behavior is attributed to the elevated water content, which impedes gas diffusion and consequently limits the penetration of CO_2 into the material, reducing the overall carbonation efficiency. Based on the results obtained, it can be concluded that, under the conditions studied, an initial w_s^0 ratio of 0.3 is optimal for maximizing carbonation of hydrated lime. In addition, the data indicates a positive correlation between the CO_2 flow rate and the TC values. Higher flow rates result in increased total carbon content. This outcome is expected, as a higher CO_2 flow rate allows the reactor to become completely fulfilled with carbon dioxide and reach a constant concentration more rapidly, thus facilitating the carbonation process.

The parameter m_{wm} refers to the mass of water remaining in the solid matrix after the carbonation process. It is calculated by comparing the mass of the aluminum cup filled with the carbonated material before and after drying at 105 °C for 12 hours. This comparison allows for the estimation of the amount of water that did not evaporate during the carbonation phase and remained retained within the matrix. The results in Table 1 show that the quantity of water retained in the solid matrix increases with the initial amount of water added, which corresponds to the w_s^0 ratio. This behavior can be explained by the distinction between evaporable and non-evaporable water during the initial hydration of calcium hydroxide. The retained water corresponds primarily to non-evaporable water, which includes chemically adsorbed water between the layers of calcium hydroxide and structurally bound water [14,16]. These results confirm that the higher the quantity of water added, the more water is chemically adsorbed in the calcium hydroxide matrix [14]. Overall, the results presented in Table 1 underscore the critical role of water in the carbonation process, emphasizing the importance of optimizing the initial water-to-solid ratio to enhance the efficiency of carbonation and maximize total carbon uptake.

2.3. Modelling work: Introduction of water evaporation into the dual scale approach

The mathematical model presented in this article addresses a dual-scale system, under the assumption that hydrated lime powder is arranged as a granular bed. To accurately model this system, it is essential to

distinguish between two scales: the macro-scale and the micro-scale. The macro-scale level represents the granular bed as a whole, while the micro-scale level focuses on the individual particles within the bed. At the macro-scale, the model calculates the bed concentration of hydrated lime based on the mass of calcium hydroxide measured experimentally, the volume of the granular bed, and the molar mass of $Ca(OH)_2$. Concurrently, the concentration of carbon dioxide above the granular bed is constant once the reactor is fully filled with pure CO_2. The granular bed is modeled as a truncated cone, which is intended to simulate the aluminum cup. The dimensions of the truncated cone are as follows: a height of 25 mm, a base diameter of 70 mm, and a top diameter of 85 mm.

On the other hand, the initial porosity of the granular bed is set at 0.65, while the particles within the bed, composed of pure calcium hydroxide, exhibit a porosity of 0.1 and a diameter of 35.5 µm. At the microscale, it is hypothesized that carbonation does not occur due to the minimal porosity and the small particle size. This assumption is supported by observations showing that, upon the initiation of carbonation, the microscale porosity rapidly decreases to zero, thereby preventing carbonation under the experimental conditions. Furthermore, the mathematical model proposed in this work assumes that the concentration of carbon dioxide above the cup is initially zero, as the reactor is filled only with air at time zero. As pure CO_2 is subsequently introduced, the concentration progressively increases until reaching a steady-state value above the cup. In addition, the water concentration at the top of the cup is assumed to correspond to air fully saturated with water vapor at 298 K, ensuring optimal mass transfer at the surface; this value is taken as 0.055 mol m^{-3}. No mass flux occurs through the walls or the bottom of the cup, as the material prevents any transfer through these boundaries. Finally, the system is considered isothermal and isobaric at 298 K and 1 bar.

Taking these assumptions into consideration, this section first presents the influence of liquid water saturation on reaction kinetics. Subsequently, the effects of the water-to-solid ratio and liquid water saturation on diffusion phenomena are discussed. Finally, the incorporation of evaporation phenomena into the modeling of water is introduced.

2.3.1. Influence of water into reaction kinetics

As previously discussed, water is a prerequisite for initiating the carbonation reaction, and its effect on the reaction kinetics is guaranteed. The kinetic rate, denoted as r (mol·mol^{-3} ·s^{-1}), is expressed as follows:

$$r = k \cdot [CO_2] \cdot [Ca(OH)_2] \quad (2)$$

where k is the kinetic constant (m^3·(mol·s)$^{-1}$), and $[CO_2]$ and $[Ca(OH)_2]$ represent the concentrations of carbon dioxide and calcium hydroxide (mol·m^{-3}), respectively. The kinetic constant is strongly influenced by the bed liquid water saturation (S_b), which corresponds to the quantity of water present in the porosity of the granular bed is quantified by the liquid water saturation parameter. The bed liquid water saturation parameter is calculated based on the water concentration, the bed porosity, and the water density [10]. This equation is an adaptation of the equation used by Thiery et. al to introduce the evaporation phenomenon [10]:

$$S_b = \frac{[w]_b \cdot M_{H_2O}(kg/mol)}{\rho_w(kg/m^3) \cdot \phi_b} \quad (3)$$

where, $[w]_b$ represents the water concentration (mol·m^{-3}), M_{H_2O} denotes the molar mass of water which is equivalent to 18 (g.mol^{-1}), ρ_w is the density of water with a value of 1000 (kg.m^{-3}) and ϕ_b is the bed porosity. Regarding Equation 3 several tendencies of these parameters can be deduced. Firstly, liquid water saturation, S_b, is directly proportional to water concentration and inversely proportional to bed porosity. A higher bed porosity results in lower liquid water saturation, as larger pores are less likely to be filled with water. Conversely, smaller pores are more susceptible to blockage and saturation. Regarding ϕ_b parameter, the variation in bed porosity due to the carbonation process is also considered in the proposed model. During the carbonation of hydrated lime, bed porosity increases due to the higher molar volume of calcium carbonate compared to calcium hydroxide [8]. This

volumetric expansion leads to an overall rise in bed porosity, which contrasts with the porosity reduction typically observed in other types of construction materials [10]. Regarding microporosity, the process of carbonation of calcium hydroxide leads to the formation of calcium carbonate within the micropores, thereby effectively blocking them and inhibiting the original porosity. Consequently, microporosity is assumed to progressively decrease to zero once carbonation begins, thereby annulling the carbonation process within the microporosity. As a result, the proposed model does not account for carbonation in the microporosity. To validate this assumption, a Mercury Intrusion Porosimetry (MIP) test was performed. The results of this test demonstrated a decrease in microporosity from 0.1 to 0.0 after 45 minutes of carbonation under specific conditions. These conditions included an initial water-to-solid ratio of 0.2, a CO_2 flow rate of 200 mL·min^{-1}, a temperature of 298 K, and atmospheric pressure.

Continuing with the kinetics, the kinetic constant remains low under conditions of limited liquid water saturation and increases with higher saturation levels, at which point diffusion governs the reaction kinetics. This dependency is described using the following piecewise function where k_0 is a base kinetic constant, equal to 0.0025 $m^3 \cdot (mol \cdot s)^{-1}$[17,18].

$$\begin{cases} k = 0 & if\ S_b < 0.05 \\ k = \dfrac{k_0 \cdot S_b}{0.275} & if\ \ 0.05 \leq S_b \leq 0.325 \\ k = k_0 & if\ S_b > 0.325 \end{cases} \quad (4)$$

The conditions defined in the piecewise function have been optimized for the specific carbonation process. Initially, a minimum liquid water saturation level of 0.05 is experimentally required for the carbonation reaction to occur. If the saturation is lower than this threshold, the reaction cannot proceed due to insufficient dissolution of the hydrated lime. Therefore, the parameter is set to zero below this value. In contrast, if liquid water saturation is higher than 0.325 the reaction achieves its maximum velocity, but is the diffusion that will stop the process as will be explained in the following section. Between these two values, the reaction kinetics follows a linear evolution.

2.3.2. Water influence in CO_2 diffusion

Following the modeling, the carbonation of hydrated lime is limited by the diffusion of CO_2 through the granular bed. The diffusion of CO_2 through the granular bed is affected by the bed porosity (ϕ_{bed}) and the bed liquid water saturation (S_b). The process is assumed to be isobaric at atmospheric pressure, due to the experimental setup in which the material is exposed to ambient pressure and the carbon dioxide is also introduced at ambient pressure. The presence of an open outlet in the setup prevents any overpressure, ensuring that the system remains at constant pressure throughout the process. On the other hand, the system is assumed to be isothermal to remain consistent with the model on which the present work is based. The equation used to determine the bed CO_2 diffusion (D_b^{CO2}) is based on the work of Belin et al. (2013), which describes the carbonation of a model material under isothermal and isobaric conditions, with no convection, and governed solely by diffusion phenomena, assuming a fast reaction rate. In their model, diffusion is characterized by Millington's correlation and it is considered at both the particle and granular bed scales ; however, the granular bed is assumed to be completely unsaturated [12,19]. In contrast, the first adaptation by Vidal de la Peña et al. (2024) does not assume saturation at either scale. In their study, at low values of liquid water saturation, the process is reaction-controlled, whereas at higher saturation levels, diffusion becomes the dominant mechanism, still within an isothermal and isobaric framework [8]. Building on these two models, this work proposes an adaptation of the diffusion equation that incorporates the influence of water evaporation into the liquid water saturation parameter, already defined above [20,21]. The modified equation is described as follows:

$$D_b^{CO2} = D_{CO_2}^0 \cdot {\phi_{bed}}^{4/3} \cdot (1 - S_b)^{10/3} \quad (5)$$

where $D^0_{CO_2}$ is the specific diffusion coefficient of CO_2 at a pressure of 0.1 MPa and a temperature of 273 K, with a value of 1.6E-5 $m^2 \cdot s^{-1}$. Following with Equation 5, it is important to characterize the liquid water saturation parameter, S_b, as it plays a key role in the diffusion phenomena. S_b is directly correlated with the water-to-solid ratio(w_s), which reflects the amount of water remaining in the solid phase after accounting for evaporation. The w_s is used to calculate S_b as it directly represents the water content in the solid phase during carbonation. Given its significant influence, the behavior of S_b is defined using a piecewise function as a function of w_s.

$$\begin{cases} S_b \approx 0 & if\ w_s \leq 0.07 \\ S_b = S_b & if\ 0.07 < w_s \leq 0.35 \\ S_b \approx 1 & if\ w_s > 0.35 \end{cases} \quad (6)$$

Regarding the piecewise function proposed in Equation 6, it is concluded that when the water-to-solid ratio w_s lower than 0.07, the granular bed is considered completely unsaturated, which results in an increase in the diffusion coefficient. Conversely, when it exceeds 0.35, the bed is assumed to be nearly fully saturated, which hinders the diffusion process. These results are in accordance with the experimental values observed in literature, as in the study done by M. Thiery et al.(2012) where they found a critical value of w_s equal to 0.45 [12]. Between these two boundaries, and in accordance with Equation 5, an increase in liquid water saturation leads to a decrease in the diffusion coefficient and conversely, a decrease in saturation leads to an increase in diffusion. Following the diffusion characterization, the proposed system also considers the diffusion of water. To characterize water diffusion in the model, the same equations used for the carbon dioxide are used, with the only difference being the standard diffusion coefficient for water at 298 K equal to 2.3 E-9 $m^2 \cdot s^{-1}$ [22].

$$D_b^{H_2O} = D^0_{H_2O} \cdot {\phi_b}^{4/3} \cdot (1 - S_b)^{10/3} \quad (7)$$

To complete the diffusion coefficients list to be used in the model, those of the solid components, $Ca(OH)_2$ and $CaCO_3$, are fixed to arbitrary low values (1 E-12 $m^2 \cdot s^{-1}$) to account for the fact that these components remain static during the carbonation process.

2.3.3. Characterization of liquid water saturation: Introduction of the water evaporation parameter

In the proposed mathematical model, water is represented by multiple parameters. Firstly, the quantity of water present in the porosity of the granular bed is quantified by the liquid water saturation parameter (S_b), as already mentioned. Subsequently, the concentration of water remaining in the granular bed $\left([w]_b\ (mol_{H_2O} \cdot m_{bed}^{-3})\right)$. Accurate modeling of the granular bed water concentration is important, as it accounts for both the production and evaporation of water, and is calculated as follows.

$$[w]_b = \frac{m_{gb}}{M_{H_2O} \cdot V_{cup}} \quad (8)$$

where, M_{H_2O} corresponds to the molar mass of water equal to 18 ($g \cdot mol^{-3}$), V_{cup} denotes the volume of the aluminum cup, which has been calculated by accounting for its geometry (m^3) and m_{gb} corresponds to the mass of water remaining in the granular bed during the carbonation process (g). The mass of water remaining in the granular bed is calculated using the following equations, where the water initially added is accounted for by the w_s^0 and m_s^0 parameters, the mass of water produced by $m_{produced}$ and the evaporated water ($m_{evaporated}$) by the w_{ev} and m_s parameters.

$$m_{gb} = w_s^0 \cdot m_s^0 + m_{produced} - m_{evaporated} \quad (9)$$

$$m_{evaporated} = w_{ev} \cdot m_s \quad (10)$$

Where, w_s^0 corresponds to the initial water-to-solid ratio (g_{H2O}/g_s), m_s^0 the mass of the solid used in the experiments (g), $m_{produced}$ to the mass of water produced during the carbonation process, w_{ev} the evaporation ratio (g_{H2O}/g_s) and m_s the solid mass after the carbonation process (g). In this model, while the experimental parameters are introduced directly, the evaporation ratio is estimated using a linear fitted equation derived from the experimental total carbon results presented in Table 1, along with the evaporation ratios obtained for each experiment, which are directly presented in Figure 2. Figure 2 illustrates this relationship, with the total carbon values plotted along the x-axis and the evaporation ratios associated on the y-axis.

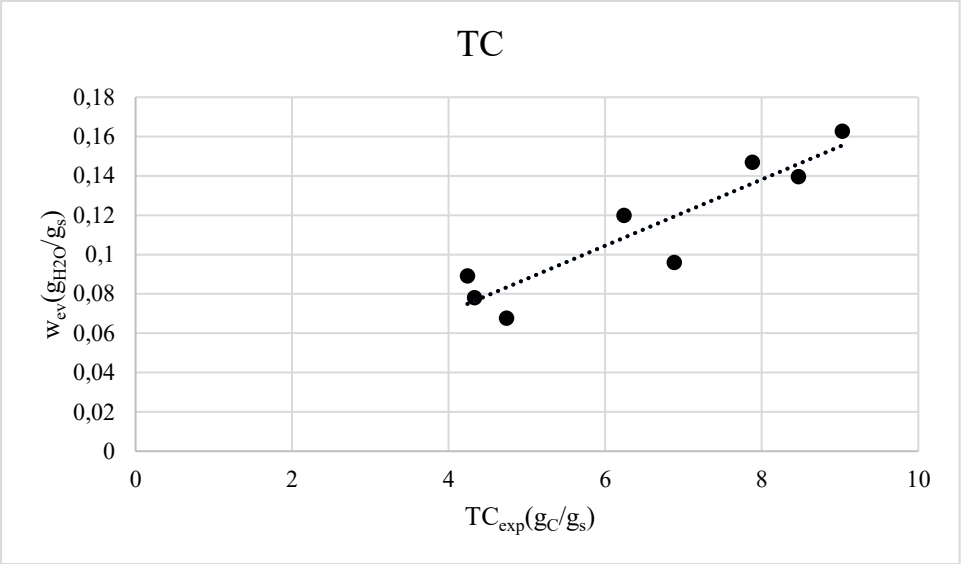

Figure 2. Linear correlation between the evaporation ratio and the total carbon content.

Regarding Figure 2, a clear trend is observed between the evaporation ratio and the final total carbon content. The higher the total carbon content, the greater the amount of water evaporated. This correlation is consistent with the exothermic nature of the carbonation reaction presented in Equation 1. However, the linear relationship does not intersect the origin, as an initial amount of energy is required to heat the solid material and the liquid phase to the temperature necessary for water evaporation. Continuing with the modeling approach, the evaporation ratio during the carbonation of hydrated lime can be summarized with the following linear correlation.

$$w_{ev} = 0.0168 \cdot TC_m + 0.0035 \tag{11}$$

Where, w_{ev} corresponds to the evaporation ratio (g_{H2O}/g_s) and TC_m corresponds to the total carbon parameter calculated by the model (g_C/g_s). In turn, the modeled total carbon parameter is calculated by first calculating the carbonation rate (η) using Equation 12.

$$\eta = \frac{[CaCO_3]}{[Ca(OH)_2]_{t=0}} \tag{12}$$

where $[CaCO_3](mol \cdot m^{-3})$ is the concentration of calcium carbonate during the process, and $[Ca(OH)_2]_{t=0}(mol \cdot m^{-3})$ is the initial concentration of calcium hydroxide, i.e. the maximum molar concentration of calcium carbonate that could be produced. Following the calculation of the carbonation rate, the total carbon is calculated by utilizing Equation 13.

$$TC = \frac{\eta * M_C}{\left(\eta * M_{CaCO_3} + (1-\eta) * M_{Ca(OH)_2}\right)} \tag{13}$$

where M_C is the molar mass of carbon and is equal to 12 ($g \cdot mol^{-1}$), M_{CaCO_3} is the molar mass of calcium carbonate with a value of 100 ($g \cdot mol^{-1}$), and $M_{Ca(OH)_2}$ is the molar mass of the calcium hydroxide which is equal to 74

($g \cdot mol^{-1}$). By considering these equations, the water balance is incorporated into the model, allowing for the consideration of the evaporation phenomenon, which is one of the main objectives of this study.

3. Results and Discussion

In this section, simulation results are shown to illustrate how the mathematical model proposed in this article works and its usefulness in understanding the carbonation process. Then, experimental results of total carbonation are presented to analyze the influence of three key parameters: the water-to-solid ratio, the CO_2 flow rate, and the carbonation duration. Afterwards, the water balances calculated from the experiments summarized in Table 1 are presented. Finally, the mathematical model proposed in this paper is validated by comparing the water balance and total carbon values calculated by the model with the experimental results.

3.1. Modelling results: CO_2 gradient, carbonation rate and liquid water saturation variation

Once the model has been coded in COMSOL Multiphysics 6.2, an investigation into an aleatory carbonation process is conducted. The parameters of the carbonation process are defined as follows: an initial water-to-solid ratio of 0.3 and a CO_2 flow rate of 200 $mL \cdot min^{-1}$. The initial material's temperature is fixed at 298 K, and the pressure is established at atmospheric pressure. The initial bed porosity is set at 0.65. The initial bed concentration is designated as 5500 mol/m^3 and it is calculated by the initial mass of the solid and the geometry of the reactor. The carbonation process is simulated for a duration of 45 minutes.

The model results are presented in Figure 3. Figure 3(a) illustrates the carbon dioxide gradient along the reactor following 45 minutes of carbonation, Figure 3(b) demonstrates the carbonation front along the reactor at three different times of carbonation. Figure 3(c) displays the volumetric liquid water saturation mean through the reactor as a function of time.

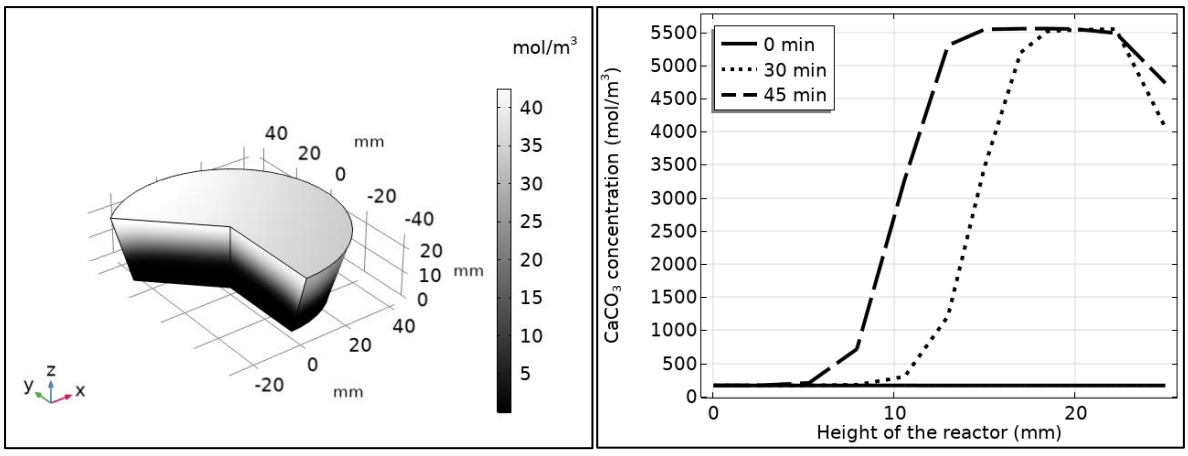

(a) (b)

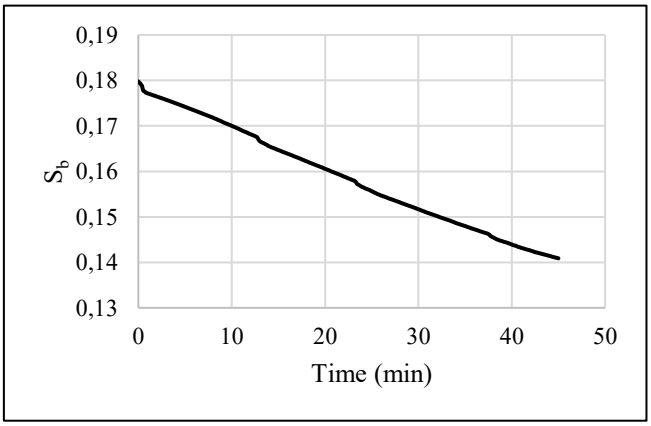

(c)

Figure 3. (a) Concentration gradient of carbon dioxide along the reactor after 45 minutes of carbonation. (b) Calcium carbonate concentration along the reactor at three different carbonation times. (c) Volumetric bed liquid water saturation mean in the reactor as a function of carbonation time.

The initial findings, illustrated in Figure 3(a), pertain to the diffusion of carbon dioxide through the granular bed. As demonstrated in Figure 3(a), the gradient of carbon dioxide concentration within the granular bed is evident, reaching its maximum concentration at the top of the aluminum cup (concentration equal to 40 $mol \cdot m^{-3}$) and lower values at the bottom of the cup (concentration equal to 5 $mol \cdot m^{-3}$). Furthermore, Figure 3(b) illustrates the concentration of calcium carbonate at various stages of carbonation within the reactor. The variable x denotes the height of the reactor, with x = 0 m representing the bottom and x = 25 mm representing the top. The variable y denotes the concentration of calcium carbonate. It is evident that the carbonation front progresses toward the base of the aluminum cup over time, reaching a constant calcium carbonate concentration of approximately 5500 $mol \cdot m^{-3}$ in the layers where carbonation is complete. At this stage, the carbonation rate would be equal to 1, considering that the maximum concentration of calcium carbonate corresponds to the initial concentration of calcium hydroxide. It is noteworthy that at the 45-minute mark, between x=0 and x=10, the layer exhibits carbonation; however, at the 30-minute marks in this region, carbonation has not yet occurred. This phenomenon is attributed to the diffusion of carbon dioxide. A comparison of Figures 3(a) and 3(b) at time 45 minutes reveals that the concentration of carbon dioxide remains low in this region. To achieve a state of complete carbonation, it is necessary to facilitate the arrival of additional carbon dioxide or just let the carbonation happen more time. This observation lends further credence to the hypothesis that, at this particular stage, the diffusion phenomenon is the predominant factor influencing the process according to the literature results [12,23–25]. In addition, the shape of the carbonation front follows the tendency found in other studies such as the one done by Thiery et al [26].

On the other hand, Figure 3(c) presents the mean volumetric bed liquid saturation in the reactor. These results are particularly relevant, as they account for the three water-related phenomena: addition, production, and evaporation. During the carbonation process, a clear decreasing trend in the liquid water saturation parameter is observed. This can be explained by several factors. First, as indicated by Equation 3, liquid water saturation is linked to porosity variations. Over time, the bed porosity increases due to the formation of calcium carbonate, leading to a continuous decrease in liquid water saturation, even though the amount of remaining water in the matrix remains constant once all evaporable water has evaporated. Secondly, the evaporation phenomenon becomes more significant than the production of water leading a decrease in the granular bed water concentration. In conclusion, the mathematical model proposed in this study effectively describes the carbonation process by accurately incorporating the three main phenomena: diffusion, carbonation reaction, and water evaporation.

3.2. Model validation: Comparison of water evaporation results and total carbon values

Following the presentation of the model and the experimental results, it is necessary to demonstrate that the model proposed in this article provides a suitable representation of the carbonation process. Given the innovative introduction of water evaporation, it is important to validate the evaporated mass of water considered by our model and the reality. To validate the model the relative error has been calculated as well as the Mean Absolute Percentage Error (MAPE) for each group of experiments classified by the carbon dioxide flux rate. To calculate the MAPE error, the following equation has been used.

$$MAPE = \frac{100\%}{n}\sum_{i=1}^{n}\left|\frac{y_i - \hat{y}_i}{y_i}\right| \quad (14)$$

where n corresponds to the total number of observations, y_i is the observed value and $\hat{y}_i$ corresponds to the predicted value. The results of the evaporated water parameter and the different error calculations are represented in Table 2.

Table 2. Validation of the evaporated water parameter: water-to-solid ratio (w_s^0), CO_2 flow rate, mass of water produced ($m_{produced}$), mass of water remaining in the matrix (m_{wm}), experimental mass of water evaporated ($m_{evaporated}$ experimental), modelled mass of water evaporated($m_{evaporated}$ model), relative error and MAPE error.

Carbonation experiment	w_s^0 (g/g)	CO_2 flow rate (mL/min)	$m_{produced}$ (g)	m_{wm} (g)	$m_{evaporated\ experimental}$ (g)	$m_{evaporated\ model}$(g)	Relative error (%)	MAPE error (%)
1	0.1	100	4.54	5.67	4.37	5.67	29.65	15.34
2	0.3	100	6.84	12.34	8.13	6.88	15.33	
3	0.4	100	5.17	16.53	6.62	6.47	2.21	
4	0.6	100	3.50	28.06	4.18	4.77	14.17	
5	0.1	200	6.94	5.95	6.49	7.56	16.51	11.14
6	0.3	200	7.98	12.57	9.67	9.00	6.90	
7	0.4	200	7.74	18.06	8.57	8.28	3.22	
8	0.6	200	3.24	25.54	4.49	5.30	17.94	

The results presented in Table 2 demonstrate a clear correlation between water evaporation and the experimental conditions. The water-to-solid ratio is a key determinant influencing water production, and consequently, the formation of calcium carbonate, in accordance with the reaction stoichiometry. Both low and high w_s^0 values result in reduced water production and evaporation. The data reveals a consistent trend indicating an optimal w_s^0 value of 0.3, as well as a positive effect of increased carbon dioxide flux on the process. To validate the model predictions, the relative errors have been calculated. As demonstrated in almost all cases, the relative error is consistently maintained below 20%, with one exception observed in experiment number 1, which can be attributed to specific experimental conditions. However, to understand the prediction of the model in relation to the initial water-to-solid ratio, the mean absolute percentage error (MAPE) has also been calculated. In all cases, the MAPE error was found to be relatively low, with higher values observed at higher CO_2 flow rate values. The findings of the validation process indicate that the model's prediction of the evaporated water parameter aligns with the experimental data. However, it is acknowledged that lower error values could be achieved if a more precise measurement of the experimental water evaporation could be obtained.

The comparison between the experimental and modeled total carbon content is shown in Figure 4. Figure 4(a) presents the model predictions for each experiment listed in Table 1, using a carbon dioxide flow rate of 100 $ml \cdot min^{-1}$, while Figure 4(b) displays the corresponding results for experiments conducted at a flow rate of 200 $ml \cdot min^{-1}$. In both bar charts, the solid white bars represent the experimental values, whereas the patterned bars correspond to the model predictions. Error bars are included to reflect experimental variability, as each test was conducted in duplicate and the total carbon content reported is the average of both measurements. The error bars represent the standard deviation between the two experimental results.

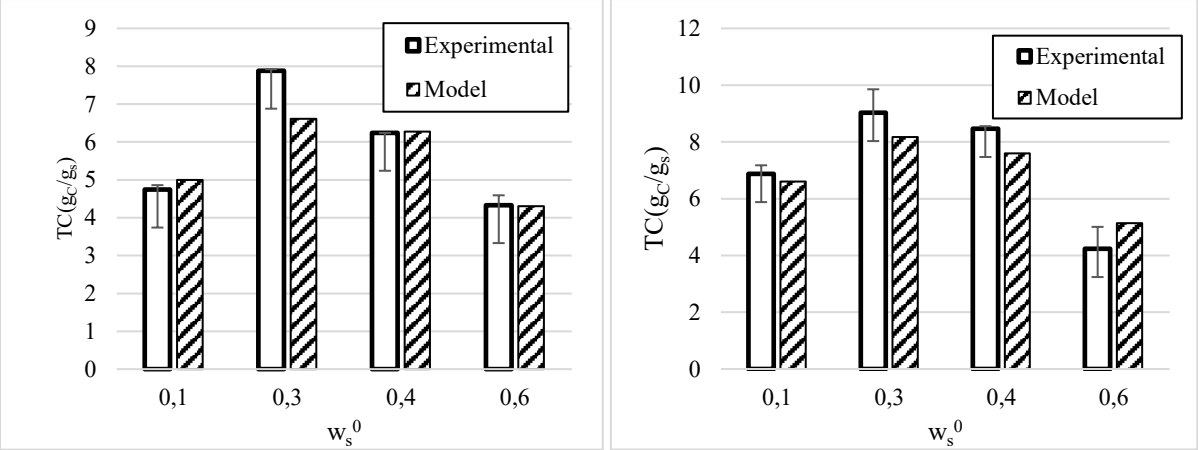

Figure 4. (a) Comparison of the total carbon results between the model and the experimental results with a CO_2 flow rate of 100 ml·min^{-1}. (b) Comparison of the total carbon results between the model and the experimental results with a CO_2 flow rate of 200 ml·min^{-1}.

With regard to Figure 4(a) and Figure 4(b), the model shows a strong correlation between the predicted and experimental values for total carbon. However, a lower degree of agreement is observed in the experiments conducted with a CO_2 flow rate of 200 mL·min^{-1}. This discrepancy can be attributed to the larger experimental uncertainty, as indicated by the error bars. A comparison of the error bars in Figures 4(a) and 4(b) reveals that the experiments at the higher flow rate exhibit greater variability, which complicates model validation at these points. Nonetheless, based on the results presented in Table 2 and Figure 4, it can be concluded that the proposed mathematical model effectively captures the carbonation process and underscores the critical role of water in this reaction.

4. Conclusion

In summary, the mathematical model proposed in this study provides a comprehensive analysis of the role of water during the carbonation process. It accounts for the three main phenomena involved in mineral carbonation: chemical reactions, diffusion processes and water evaporation. Furthermore, it has been demonstrated that during carbonation, the evaporation mechanism accounts for all the water produced and a portion of the water added, referred to as evaporable water. An experimental fitting equation is provided to predict the evaporation ratio. The proposed model accurately predicts the mass of water evaporated under different carbonation conditions and offers a reliable estimation of the total carbon present in the material after various carbonation experiments. Consequently, the mathematical model presented in this study provides a deeper understanding of the role of water in the process, contributing to the overall knowledge of mineral carbonation. This, in turn, supports the broader objective of promoting a circular economy in the construction sector.

Author contributions: Conceptualization, N.V, S.M, S.J, D.T and G.L; Methodology and validation, N.V; Software, N.V, D.T and G.L; Formal analysis, N.V, D.T and G.L; Investigation, Data curation, Writing, N.V, D.T and G.L; Supervision, D.T and G.L; Project administration, G.L; Funding acquisition, Walloon Region Mineral Loop project.

Funding sources : This research was financed by the Mineral Loop project, funded by the Walloon Region through the Greenwin Competitiveness Cluster (C8505).

Conflicts of Interest: The authors declare no conflict of interest.

Acronyms:

w_s^0: initial water-to-solid ratio (g_{H2O}/g_s)
m_s^0: initial solid mass (g)
m_{wm}: mass of water remaining in the solid matrix after carbonation (g)
S_b: bed liquid water saturation

$m_{evaporated}$: mass of water evaporated (g)
m_{gb}: mass of water remaining in the granular bed (g)
$m_{produced}$: mass of water produced (g)
$[w]_b$: concentration of water in the granular bed ($mol.m^{-3}$)
η: carbonation rate
TC: total carbon (g_C/g_s)
w_{ev}: evaporation ratio (g_{H2O}/g_s)
m_s: mass of solid material (g)
ϕ_b: bed porosity

References

[1] Eurostat, Waste generation by economic activities and households, EU, 2022, Waste Generation by Economic Activities and Households, EU, 2022 (n.d.). https://doi.org/10.2908/ENV_WASGEN (accessed December 12, 2024).

[2] European Comission, The European Green Deal, (n.d.). https://commission.europa.eu/strategy-and-policy/priorities-2019-2024/european-green-deal_en (accessed December 9, 2024).

[3] Greenwin, MINERAL LOOP, (n.d.). https://www.greenwin.be/fr/successStory/consult/37 (accessed December 9, 2024).

[4] F.C. Fonseca, J. Cárcel-Carrasco, A. Preciado, A. Martínez-Corral, A.S. Montoya, Comparative Analysis of the European Regulatory Framework for C&D Waste Management, Advances in Civil Engineering 2023 (2023). https://doi.org/10.1155/2023/6421442.

[5] A. Bourchy, S.A. Saslow, B.D. Williams, N.M. Avalos, W. Um, N.L. Canfield, L. Sweet, G.L. Smith, R.M. Asmussen, The evolution of hydrated lime-based cementitious waste forms during leach testing leading to enhanced technetium retention, J Hazard Mater 430 (2022). https://doi.org/10.1016/j.jhazmat.2022.128507.

[6] A. Sanna, M. Uibu, G. Caramanna, R. Kuusik, M.M. Maroto-Valer, A review of mineral carbonation technologies to sequester CO2, Chem Soc Rev 43 (2014) 8049–8080. https://doi.org/10.1039/c4cs00035h.

[7] Natalia Vidal-De La Peña, Sophie Grigoletto, Dominique Toye, Luc Courard, Grégoire Léonard, CO2 capture by mineral carbonation of construction and industrial wastes., in: Francisco M. Baena-Moreno, Judith González-Arias, Tomás Ramírez-Reina, Laura Pastor-Pérez (Eds.), Circular Economy Processes for CO2 Capture and Utilization, First, Elsevier, 2023.

[8] N. Vidal de la Peña, S. Marquis, S. Jacques, E. Aubry, G. Léonard, D. Toye, A Mathematical Model for Enhancing CO2 Capture in Construction Sector Using Hydrated Lime, Minerals 14 (2024) 889. https://doi.org/10.3390/min14090889.

[9] A. Morandeau, M. Thiéry, P. Dangla, Investigation of the carbonation mechanism of CH and C-S-H in terms of kinetics, microstructure changes and moisture properties, Cem Concr Res 56 (2014) 153–170. https://doi.org/10.1016/j.cemconres.2013.11.015.

[10] M. Thiery. Modelling of atmospheric carbonation of cement based materials considering the kinetic effects and modifications of the microstructure and the hydric state. Engineering Sciences [physics]. Ecole des Ponts ParisTech, 2005. English. ffNNT : ff. ffpastel-00001517.

[11] M.J. Mitchell, O.E. Jensen, K.A. Cliffe, M.M. Maroto-Valer, A model of carbon dioxide dissolution and mineral carbonation kinetics, Proceedings of the Royal Society A: Mathematical, Physical and Engineering Sciences 466 (2010) 1265–1290. https://doi.org/10.1098/rspa.2009.0349.

[12] M. Thiery, P. Dangla, P. Belin, G. Habert, N. Roussel, Carbonation kinetics of a bed of recycled concrete aggregates: A laboratory study on model materials, Cem Concr Res 46 (2013) 50–65. https://doi.org/10.1016/j.cemconres.2013.01.005.

[13] Ö. Cizer, C. Rodriguez-Navarro, E. Ruiz-Agudo, J. Elsen, D. Van Gemert, K. Van Balen, Phase and morphology evolution of calcium carbonate precipitated by carbonation of hydrated lime, J Mater Sci 47 (2012) 6151–6165. https://doi.org/10.1007/s10853-012-6535-7.

[14] X. Willem, A. Darimont, R. Degeimbre, and L. Courard. "Etude de la consolidation du béton frais sur base de la porosité à l'état durci." In Compte-rendu des Journées Scinetifiques du (RF)2Bedited by L. Courard. 2004.

[15] F. Gendron, Carbonatation des matériaux cimentaires : étude de la diffusion du CO2, n.d. https://theses.hal.science/tel-02520206v1.

[16] N. Pingintha, M.Y. Leclerc, J.P. Beasley, G. Zhang, C. Senthong, Assessment of the soil CO2 gradient method for soil CO2 efflux measurements: Comparison of six models in the calculation of the relative gas diffusion coefficient, Tellus B Chem Phys Meteorol 62 (2010) 47–58. https://doi.org/10.1111/j.1600-0889.2009.00445.x.

[17] L. Reich, L. Yue, R. Bader, W. Lipiński, Towards solar thermochemical carbon dioxide capture via calcium oxide looping: A review, Aerosol Air Qual Res 14 (2014) 500–514. https://doi.org/10.4209/aaqr.2013.05.0169.

[18] F. Fang, Z. shan Li, N. sheng Cai, CO2 capture from flue gases using a fluidized bed reactor with limestone, Korean Journal of Chemical Engineering 26 (2009) 1414–1421. https://doi.org/10.1007/s11814-009-0198-3.

[19] R.J. Millington, Gas Diffusion in Porous Media, 1959.

[20] Z. Li, L. Yuan, G. Sun, J. Lv, Y. Zhang, Experimental determination of co2 diffusion coefficient in a brine-saturated core simulating reservoir condition, Energies (Basel) 14 (2021). https://doi.org/10.3390/en14030540.

[21] N. Pingintha, M.Y. Leclerc, J.P. Beasley, G. Zhang, C. Senthong, Assessment of the soil CO2 gradient method for soil CO2 efflux measurements: Comparison of six models in the calculation of the relative gas diffusion coefficient, Tellus B Chem Phys Meteorol 62 (2010) 47–58. https://doi.org/10.1111/j.1600-0889.2009.00445.x.

[22] I.N. Tsimpanogiannis, O.A. Moultos, L.F.M. Franco, M.B. de M. Spera, M. Erdős, I.G. Economou, Self-diffusion coefficient of bulk and confined water: a critical review of classical molecular simulation studies, Mol Simul 45 (2019) 425–453. https://doi.org/10.1080/08927022.2018.1511903.

[23] B. Hökfors, M. Eriksson, E. Viggh, Modelling the cement process and cement clinker quality, Advances in Cement Research 26 (2014) 311–318. https://doi.org/10.1680/adcr.13.00050.

[24] F. Gendron, Carbonatation des matériaux cimentaires : étude de la diffusion du CO2, 2019. https://theses.hal.science/tel-02520206.

[25] H. Cui, W. Tang, W. Liu, Z. Dong, F. Xing, Experimental study on effects of CO2 concentrations on concrete carbonation and diffusion mechanisms, Constr Build Mater 93 (2015) 522–527. https://doi.org/10.1016/J.CONBUILDMAT.2015.06.007.

[26] M. Thiery, G. Villain, P. Dangla, G. Platret, Investigation of the carbonation front shape on cementitious materials: Effects of the chemical kinetics, Cem Concr Res 37 (2007) 1047–1058. https://doi.org/10.1016/J.CEMCONRES.2007.04.002.